

Dedicated to Professor Bogdan C. Simionescu  
on the occasion of his 70th anniversary

## POROUS POLY(N-ISOPROPYLACRYLAMIDE-CO-HYDROXYETHYLACRYLAMIDE) HYDROGELS FOR CONTROLLED DELIVERY OF DRUGS

Sanda BUCĂȚARIU, Marieta CONSTANTIN and Gheorghe FUNDUEANU\*

“Petru Poni” Institute of Macromolecular Chemistry, Gr. Ghica Vodă Alley 41A, 700487, Iași, Romania

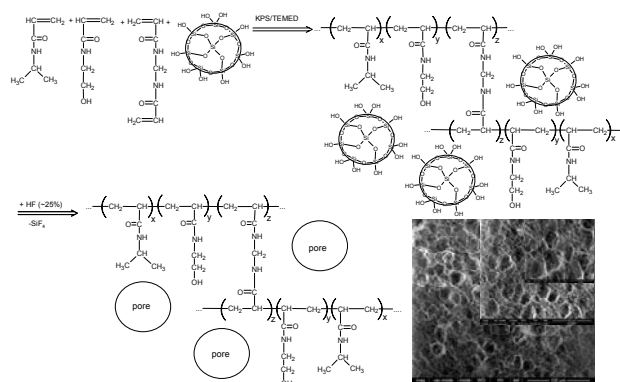
Received July 28, 2017

It is well-known that the swelling/deswelling rates of thermosensitive hydrogels are deeply influenced by their porosity. In this respect, porous thermosensitive hydrogels (PHs) with a lower critical solution temperature around the human body temperature were prepared by copolymerization of N-isopropylacrylamide (NIPAAm) with hydroxyethylacrylamide (HEAAm) in the presence of silica microspheres (SiMs) with a diameter of 7  $\mu\text{m}$ . Subsequently, SiMs were removed by solubilization in aqueous HF solution (20%, v/v) for 48h at ambient temperature. Control hydrogels in the absence of SiMs were prepared in similar conditions.

For both types of hydrogels, the morphology, swelling behavior, temperature sensitivity, and drug release profiles were investigated.

It was proved that the swelling/collapsing rate of porous hydrogel was significantly enhanced compared to conventional hydrogel and was easily controllable by adjustments in the amount of SiMs.

In addition, the release rate of metoclopramide, taken as model drug, was deeply influenced by the temperature and the porosity of the hydrogel.



### INTRODUCTION

Hydrogels are crosslinked three dimensional networks of hydrophilic polymer chains.<sup>1,2</sup> They have been used extensively in the development of soft material with applications in both chemical and technological fields.<sup>2</sup> The most widely used polymer to obtain smart thermosensitive hydrogels is poly(N-isopropylacrylamide) (PNIPAAm), which has a lower critical solution temperature (LCST) of ca. 32 °C in aqueous solutions.<sup>3</sup> Therefore, it is

hydrophilic below the LCST, and above the LCST becomes hydrophobic because of its chain conformation changes. Accordingly, the hydrogels obtained from this polymer have a critical temperature, called volume phase transition temperature (VPTT). Below the VPTT, these hydrogels are in the swollen state, while above VPTT they undergo a volume transition and collapse.<sup>3,4</sup> This dramatic reduction in volume is due to water expulsion during collapse.<sup>5</sup> Usually, for homogeneous hydrogel samples, the swelling

\* Corresponding author: ghefun@icmpp.ro

rate is slower than the deswelling rate, the response rate being controlled by solvent diffusion. This is dependent on the shape and volume of the hydrogels. However, the expulsion of water molecules is sometimes suppressed by the formation of a denser layer on the surface of collapsed hydrogel, so-called "skin effect".<sup>6</sup> Therefore, the deswelling rate could be enhanced by the formation of micrometer-sized pores in hydrogels. In the past few years, there has already been reported the preparation of porous hydrogels by addition of pore forming agents,<sup>7,9</sup> polymerization of phase separated systems above the LCST,<sup>10</sup> incorporation of dendrimers,<sup>11</sup> introduction of side chains<sup>12</sup> and so on. A research group has reported the preparation of porous PNIPAAm hydrogels by incorporation of polyhedral silica particles and the subsequent acid extraction of it.<sup>2</sup> The deswelling rate was increased by 80 times that of conventional hydrogels.

In our study, porous hydrogels were prepared by free radical co-polymerization of NIPAAm with HEAAm in the presence of variable amounts of silica microspheres (7  $\mu\text{m}$  diameter) and the subsequent extraction from microspheres with HF. Thus, we obtained novel poly(NIPAAm-co-HEAAm) hydrogels with micrometer-sized pores with an improved deswelling rate in comparison with conventional hydrogels. The deswelling behavior of the hydrogels was analyzed by temperature change from 25 (below VPTT) to 50  $^{\circ}\text{C}$  (above VPTT). The reverse process was also analyzed to evaluate the reversibility of swelling behavior. *In vitro* release studies of metoclopramide were performed in simulated physiological conditions above the VPTT, and it was obtained a prolonged time of release.

## EXPERIMENTAL

### 1. Materials

N-isopropylacrylamide (NIPAAm), from Sigma-Aldrich Chemie GmbH. (Germany), was recrystallized from hexane. Hydroxyethylacrylamide (HEAAm) from Aldrich (Germany), potassium persulfate (KPS), N,N'-methylenebisacrylamide (BIS), N,N,N',N'-tetramethylethylenediamine (TEMED) from Fluka (Germany), have been used as received. Daisogel microparticles (7  $\mu\text{m}$  diameter and 100 nm pores) were purchased from Daiso Co. (Japan). Metoclopramide (Met) was purchased from Sigma-Aldrich Chemical Co. (St. Louis, USA). Standard phosphate buffer solution (PBS) at pH =7.4 (50 mM  $\text{Na}_2\text{HPO}_4 + \text{NaOH}$ ) was prepared in our laboratory.

### 2. Methods

#### 2.1. Composite hydrogels preparation

The synthesis of composite hydrogels (CHs) was performed as follows: 1.13 g of NIPAAm (10 mmol), 0.23 g of HEAAm (2 mmol) and 0.0075g BisAAm (0.048 mmol; 0.4% mol BisAm vs. monomers) were dissolved in 7 mL

distilled water. After complete dissolution, various amounts of silica microspheres (SiMs) (0-10%, SiMs/solvent) were suspended in solution and the mixture was left in the vacuum oven for an hour, at room temperature, in order to remove and replace the air from SiMs pores with monomers solution. Dry nitrogen was bubbled through the solution for 45 min before polymerization. Next, the initiator (0.027g, 0.26 mmol of KPS; 2.2% mol KPS vs monomers) was added and kept for 5 minutes under nitrogen atmosphere to generate free radicals. Finally, the polymerization accelerator (100  $\mu\text{L}$  of TEMED) was added, the mixture was homogenized, and then quickly transferred into a 10 mL syringe. After, the syringe was slowly shaken (up and down) for homogenous distribution of the SiMs. In order to obtain the complete polymerization of the CHs, the reaction mixture was left into syringe for 24 hours. The resulting samples were removed from the syringe and cut into cylinder-like pieces approximately 15 mm in diameter and 10 mm in thickness.

In order to obtain porous hydrogels, the silica was subsequently extracted in an aqueous 23 wt % HF solution through immersion of the CHs for 24 h at ambient temperature. Finally, all the hydrogel samples were washed three times with distilled water at room temperature and were recovered by drying at room temperature, for the subsequent studies, or lyophilized for morphological and dimensional analysis. Similar preparation conditions were used for the synthesis of conventional hydrogels, without SiMs within the polymer network.

#### 2.2. Scanning Electron Microscopy (SEM) analysis

For SEM analysis, hydrogels were quickly frozen in liquid nitrogen and then dried in vacuum ( $-57^{\circ}\text{C}$ ,  $5.5 \times 10^{-4}$  mbar) for 48 h. Dried hydrogels were carefully fractured and the interior morphology was observed by an Environmental Scanning Electron Microscope (ESEM), typeQuanta 200, operating with secondary electrons in Low Vacuum, at 20 kV.

### 2.3. Swelling studies

#### 2.3.1. Temperature dependence of swelling ratios

The swelling ratio (SR) of hydrogel sample was determined over 25-60  $^{\circ}\text{C}$  range with 3-4  $^{\circ}\text{C}$  increments, using thermostated water bath. The dry hydrogel samples were weighed and equilibrated in excess of swelling medium for at least 12 h for each predetermined temperature.<sup>13</sup> Then, the hydrogels were removed from medium, and weighed after blotted with moistened filter paper to remove the solution excess on the surface. The SR was calculated according to the following equation:

$$\text{SR} = (W_s - W_d) / W_d$$

where  $W_s$  is the weight of swollen hydrogels at each temperature and  $W_d$  is the weight of dry hydrogel. The dry weights of samples were obtained after drying at room temperature followed by vacuum drying for at least 24 h.

The VPTT of the hydrogels was determined as the inflexion point of obtained curves which represented the swelling ratio as function of temperature.

#### 2.3.2. Swelling kinetics

The dry hydrogel sample was weighed and then immersed in an excess of distilled water at room temperature (25  $^{\circ}\text{C}$ ). Then, the hydrogel was removed from medium at various time intervals and weighed after the excessive solution on the surface was blotted with moistened filter paper. The swelling ratio was calculated for three samples of each hydrogel.

### 2.3.3. Deswelling kinetics

The samples were swollen in distilled water, at room temperature until the equilibrium was reached. The equilibrated samples were quickly transferred to hot solutions at 50 °C. At predetermined time interval, the samples were removed and weighed after wiping off the excess solution on the surface with a filter paper. The following equation was used to determine the water retention capacity (WR) as a function of time:

$$WR_t = (W_t - W_d) \times 100 / (W_s - W_d)$$

where  $W_d$  is the weight of the dried hydrogel,  $W_s$  is the weight of the swollen hydrogel at equilibrium (25 °C), and  $W_t$  is the weight of the hydrogel at various exposure times.

### 2.3.4. Swelling/deswelling reversibility studies

The swelling/deswelling reversibility studies of hydrogels were performed by immersing the samples in distilled water alternatively at 25 °C and 50 °C for 2 hours at each temperature. The swelling/deswelling behavior was evaluated in terms of swelling ratio.

### 2.4. Drug loading and release studies

For loading Met, each dried hydrogel sample was immersed in 10 mL of drug aqueous solution (2 mg/mL), and maintained soaked for seven days at 4 °C. Then, the drug loaded-samples were removed and washed with distilled water and dried at room temperature in a vacuum oven. The amount of Met remained in the collected solutions was determined by the UV measurements using a previously made calibration curve. The amount of Met loaded in each sample was determined according to the following equation:

$$\text{Met}_{\text{loaded}} = [\text{Met}]_i - [\text{Met}]_f$$

where  $[\text{Met}]_i$  and  $[\text{Met}]_f$  are the Met concentration in the solution before and after the loading process, respectively.

The Met release studies were performed by immersing Met loaded hydrogels (about 0.150-0.200 g containing ca 3-4 mg of Met) in PBS (pH=7.4) at 37 °C. At predetermined time intervals, 3.0 mL of the release solution was taken out and the Met concentration was determined spectrophotometrically at

272 nm, using a previously made calibration curve. The same volume of fresh release medium was added to keep unchanged the volume of release system.

## RESULTS AND DISCUSSION

### 1. Composite hydrogels preparation

The hydrogels were prepared by free radical polymerization of NIPAAm and HEAAm at a molar ratio of 10:2. This value was already established by Fundeanu *et al.* (2013)<sup>14</sup> that obtained a linear copolymer [poly(NIPAAm-co-HEAAm)] with a LCST value close to that of the human body.

Some particles may influence the polymerization reaction leading to lower yields of hydrogel samples.<sup>16</sup> Therefore, particular attention must be given to the preparation of the poly(NIPAAm-co-HEAAm) hydrogels with variable silica microspheres content, although porous PNIPAAm hydrogels were successfully obtained in the presence of silica particles with nano<sup>15</sup> or micrometer<sup>16</sup> in size. This is a good indication that silica particles did not influence the radical polymerization of NIPAAm. In this study, poly(NIPAAm-co-HEAAm) hydrogels were prepared with silica microspheres with a diameter of 7 µm at variable percent in the reaction mixture.

The preparation conditions of conventional and composite hydrogels are presented in **Table 1**. The hydrogels were successfully prepared with an yield of 75-85% even with variable amounts of silica. It was demonstrated by Takeshi Serizawa<sup>16</sup> that the structure of polymer is not damaged under the acidic conditions. The synthesis steps of porous hydrogels are shown in **Fig. 1**.

Table 1

Feed compositions used in synthesis of hydrogels

Sample code	NIPAAm (mmol)	HEAAm (mmol)	BisAAm (mol % to monomers)	Silica			Yield (%) <sup>d</sup>
				mg	% to water	% to monomer	
H <sup>a</sup>	10	2	0.4	-	-	-	84.5
CHSi <sub>2</sub> <sup>b</sup>	10	2	0.4	150	2	11	82.12
CHSi <sub>6</sub>	10	2	0.4	420	6	30	78.6
CHSi <sub>10</sub>	10	2	0.4	700	10	51	76.32
p <sub>2</sub> H <sup>c</sup>	10	2	0.4	0 <sup>e</sup>	-	-	-
p <sub>6</sub> H	10	2	0.4	0	-	-	-
p <sub>10</sub> H	10	2	0.4	0	-	-	-

<sup>a</sup>H – notation for conventional hydrogel. <sup>b</sup>CHSi<sub>x</sub> – notation for composite hydrogels where x means the percentage of SiMs relative to distilled water used in the polymerization mixture. <sup>c</sup>p<sub>x</sub>H – notation for porous hydrogels where x has the same meaning as for composite hydrogels. <sup>d</sup>The yield was determined by the ratio between dry weight of the obtained hydrogel and total amount of monomer and SiMs in the feed. <sup>e</sup>The silica microspheres was totally removed after HF treatment of CHSi hydrogels, proved by SEM and FTIR (not shown).

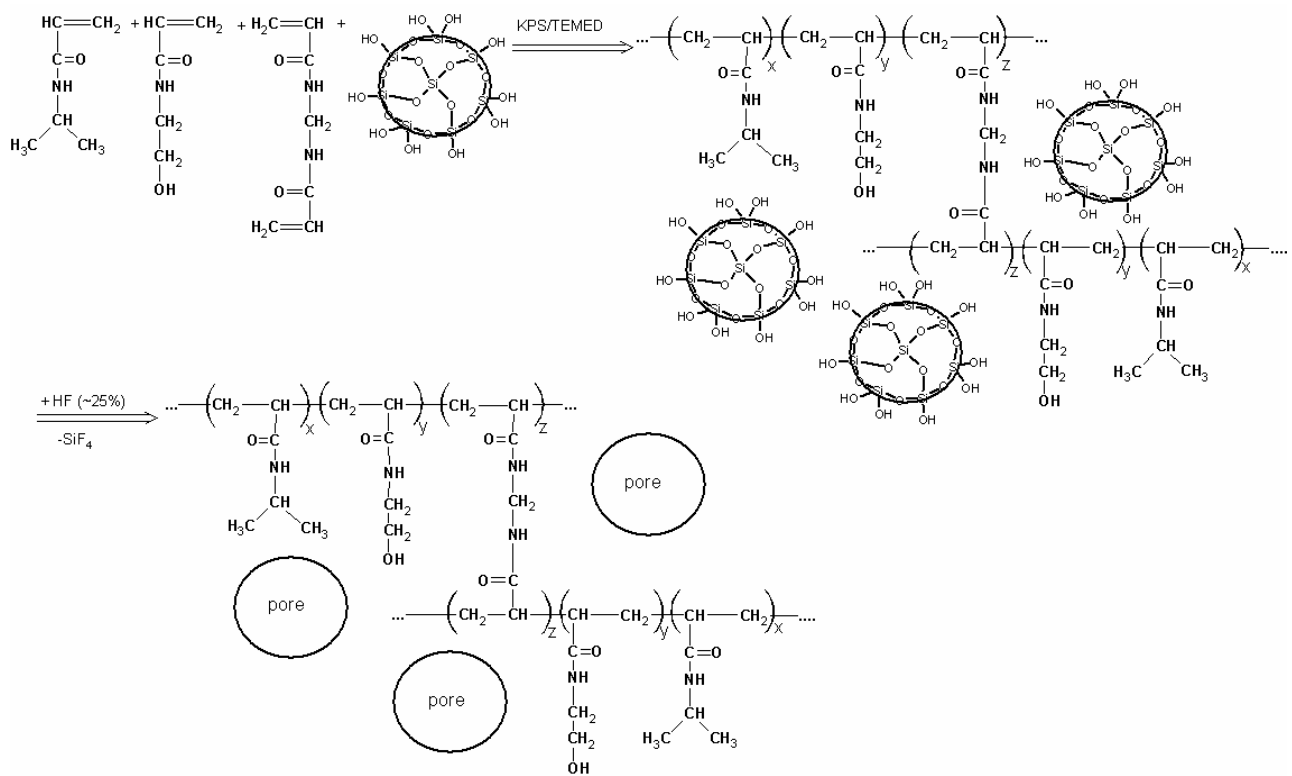


Fig. 1 – Schematic representation of the synthesis steps of porous hydrogels.

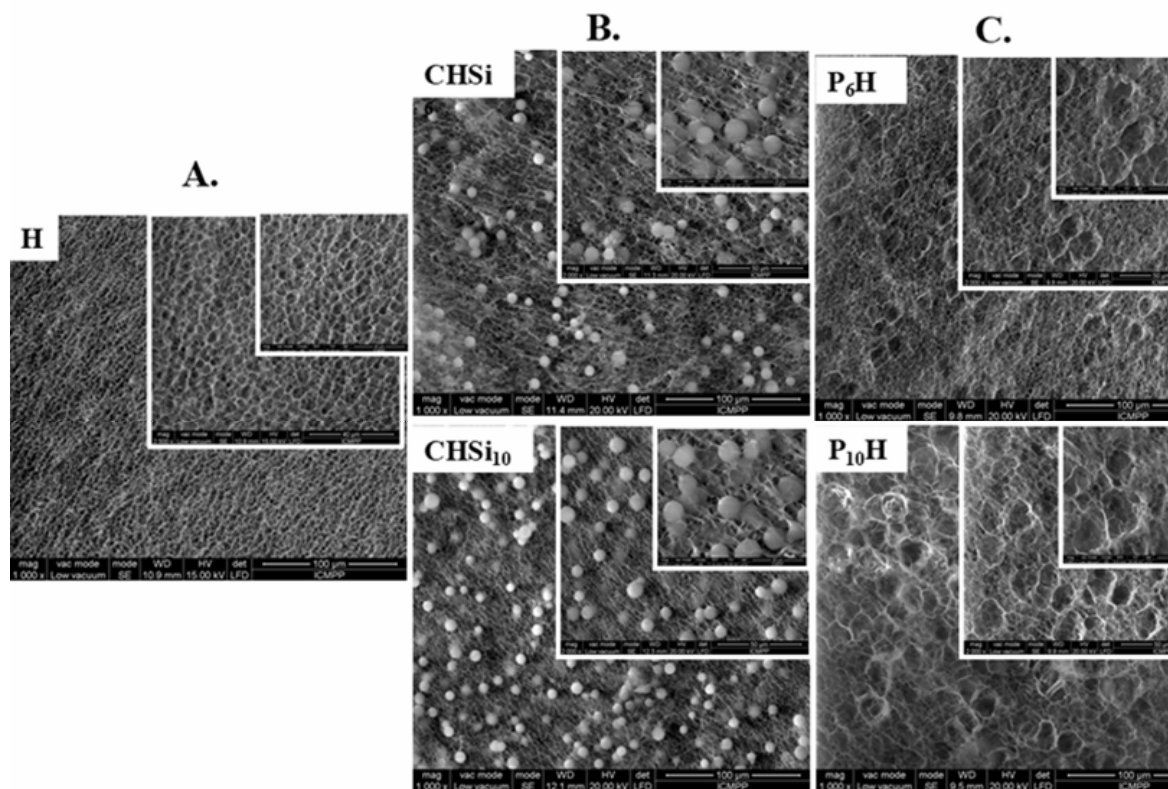


Fig. 2 – Scanning electron micrographs of conventional hydrogel (A), silica-incorporated composite hydrogels (B) and porous hydrogel after removal of SiMs (C).

## 2. Morphological analysis

Morphologies of conventional and composite hydrogels were determined by SEM (Fig. 2). In order to have images with hydrogels in their natural state, the samples were first swollen in distilled water, then frozen and lyophilized. As shown in **Fig. 2A**, even hydrogels prepared in the absence of SiMs display a certain porosity. The incorporation of SiMs was successfully performed, however the distribution of particles was not completely homogeneous (**Fig. 2B**). Porous structures were clearly observed after the treatment with HF. The pores density was dependent on the amount of silica particles (**Fig. 2C**). It must be noticed that a fraction of monomers copolymerizes within the pores of SiMs, therefore the resulted pores are not completely empty after silica removal.

## 3. Thermosensitive properties

### 3.1. Determination of VPTT at equilibrium

From the viewpoint of biomedical applications, the most important characteristic of the PNIPAAm hydrogels is the rapid change in swelling degree, and hence of the sample volume at a temperature close to that of the human body.<sup>6</sup>

The swelling ratio (SR) of poly (NIPAAm-co-HEAAm) based hydrogels in PBS over a temperature range from 25 to 60 °C is shown in **Fig. 3**. All hydrogels presented a general switch from relatively large swelling to deswelling at

around 33 °C. VPTT represents the inflection point of the curve which was obtained from the SR variation as function of temperature. It is apparent that the phase transition temperature was slightly affected by the embedded SiMs and by the pores obtained after dissolution of SiMs with HF.

As it can be seen from **Fig. 3A**, all composite hydrogels, under the VPTT value, had a lower swelling ratio than that of conventional ones because of the formation of hydrogen bonds between amide groups from the polymeric network and silanol groups from silica surface, demonstrating that silica particles could act like a cross-linker. This behaviour was underlined by the decrease of swelling ratio with the increase of the concentration of silica microspheres inside the hydrogel.

Above VPTT, hydrogen bonds break but the water diffusion from silica microspheres pores is blocked because of the fast collapsing of hydrogel. As a result, the deswelling capacity of hydrogel decreased with the increasing silica content in hydrogel. Under the VPTT value (**Fig. 3B**) the swelling ratios of porous hydrogels are lower than in the case of conventional hydrogel, being almost linear. Also, under VPTT, the swelling ratios of porous hydrogels decreased with the increase of the porosity of hydrogel. Comparing the VPTT values of porous and conventional hydrogels it was observed a decrease of this value with about two units for porous hydrogels.

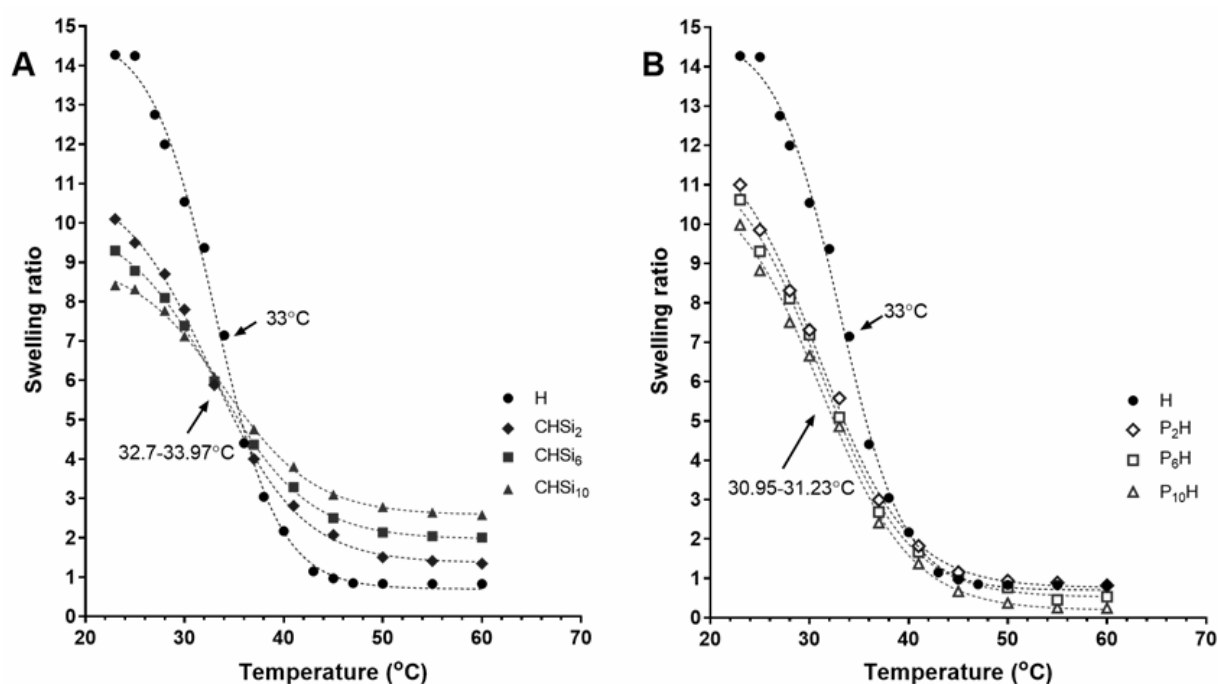


Fig. 3 – Swelling ratios of hydrogels as function of temperature.

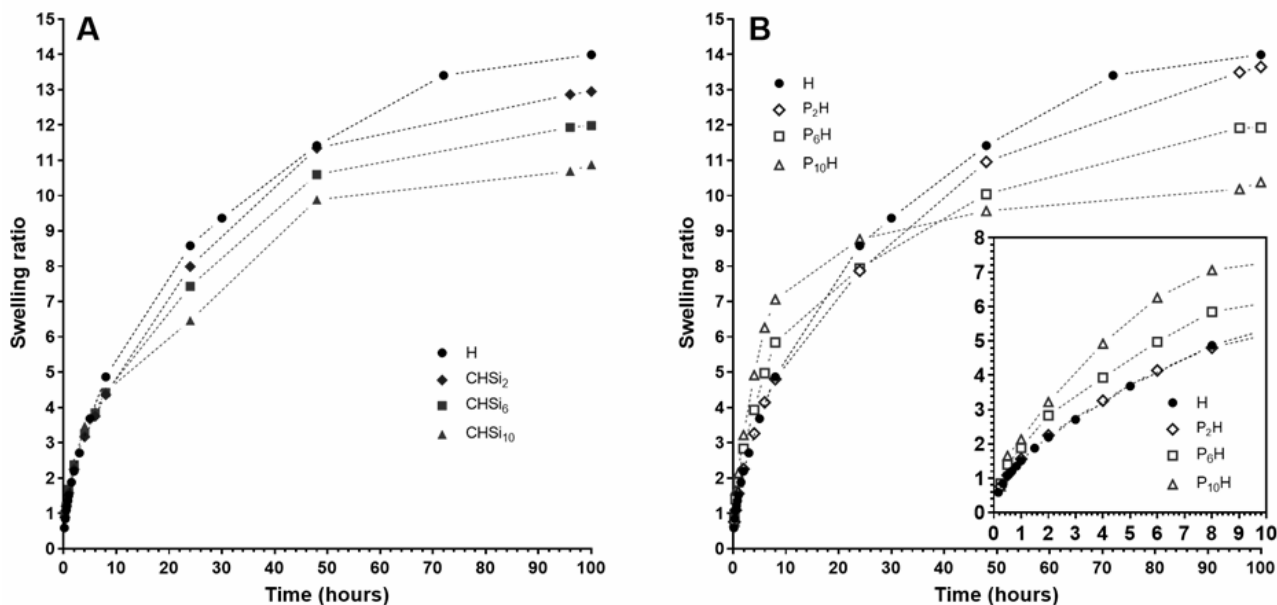


Fig. 4 – Swelling kinetic curves of composite (A) and porous (B) hydrogels in comparison with conventional one (sample H) in phosphate buffer solution at pH=7.4 at 25 °C.

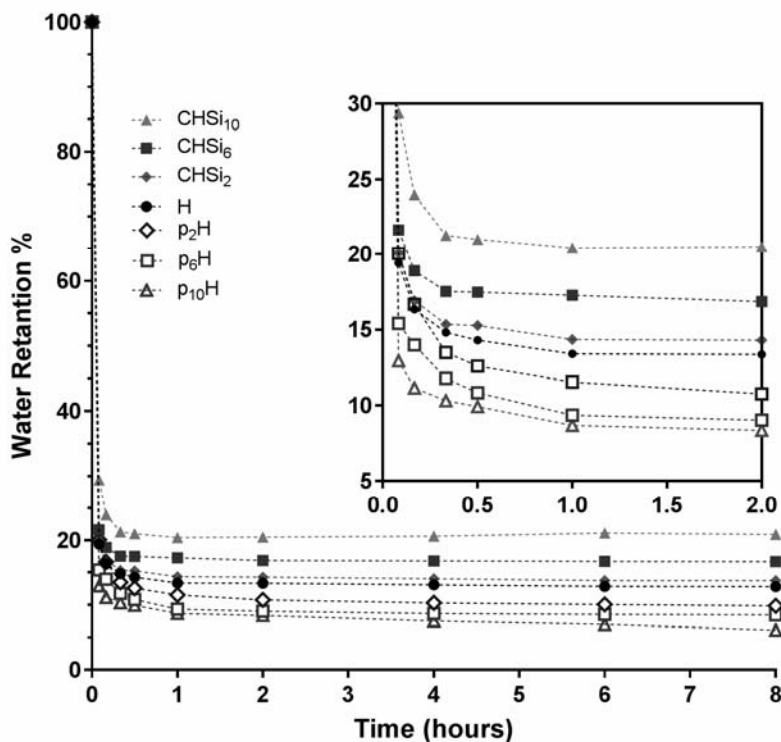


Fig. 5 – Water retention in hydrogels as function of time.

### 3.2. Swelling kinetics

One of the most important characteristics of thermosensitive hydrogels used for biomedical applications is the response rate to small changes of the temperature. Therefore, swelling kinetics of hydrogels was investigated in relation with

temperature and the amount of incorporated silica microspheres.

In *Fig. 4* is shown the swelling kinetics in water at 25 °C (under VPTT) of the composite (A) and porous hydrogels (B). In the first 8 hours, for composite hydrogels, the silica microspheres do not seem to

have any influence on the swelling ratio. However, composite hydrogels have lower swelling ratios when they reach equilibrium because of silica particles which act like a cross-linker. Instead, in the case of porous hydrogels, swelling occurs rapidly in the first hours after which the rate of swelling increases slowly until reaching equilibrium. It must be mentioned that equilibrium swelling ratios are lower for hydrogels with increased porosity. The loss of swelling capacity may be due to a larger three-dimensional mesh.

### 3.3. Deswelling kinetics

Basically, the deswelling rate of hydrogels is a result of the water diffusion from three-dimensional polymeric network, a process which depends on the network porosity. At large hydrogel porosity the water diffusion is rapid, and as a consequence the responsivity of hydrogel to the temperature is faster. Due to the porous structure of hydrogels the deswelling process took place rapidly at temperatures above VPTT.

From **Fig. 5** it can be observed that the water content for all hydrogels dropped down under 50% in the first 10 min. At equilibrium, hydrogels obtained after silica removal had the water content below 10% comparing with 15% for conventional and composite hydrogels. This fact could be attributed to the pores created after the silica removal with HF, which makes the hydrogel

network more compressible than conventional hydrogels. In the case of composite hydrogels, the water content did not fall under 15% because of the presence of water within the pores of silica that is not expelled during the collapsing process.

### 3.4. Swelling/deswelling reversibility studies

When biomedical applications are concerned, one of the major requirements of the porous hydrogels is a fast swelling/collapsing rate whenever small temperature change occurred.

**Fig. 6** shows the swelling reversibility of the hydrogel between 25 °C and 50 °C. All hydrogels were able to swell upon temperature changes from 50 to 25 °C and collapse quickly when temperature changes from 50 to 25 °C. It can be observed that the swelling/deswelling processes of hydrogels are reversible being in agreement with the temperature changes. As expected, the more porous is the hydrogel, the higher is the difference between the swelling ratios at the two extreme temperatures (25 and 50 °C) (**Fig. 6B**). It can be also noticed that the collapsing rate is higher than the swelling one because the water is ejected mechanically during the collapse of hydrogel. The structure of the hydrogel with large numbers of pores was favorable for easy diffusion of the swelling fluid into the polymeric matrix, thus contributing to its quick response toward temperature change.

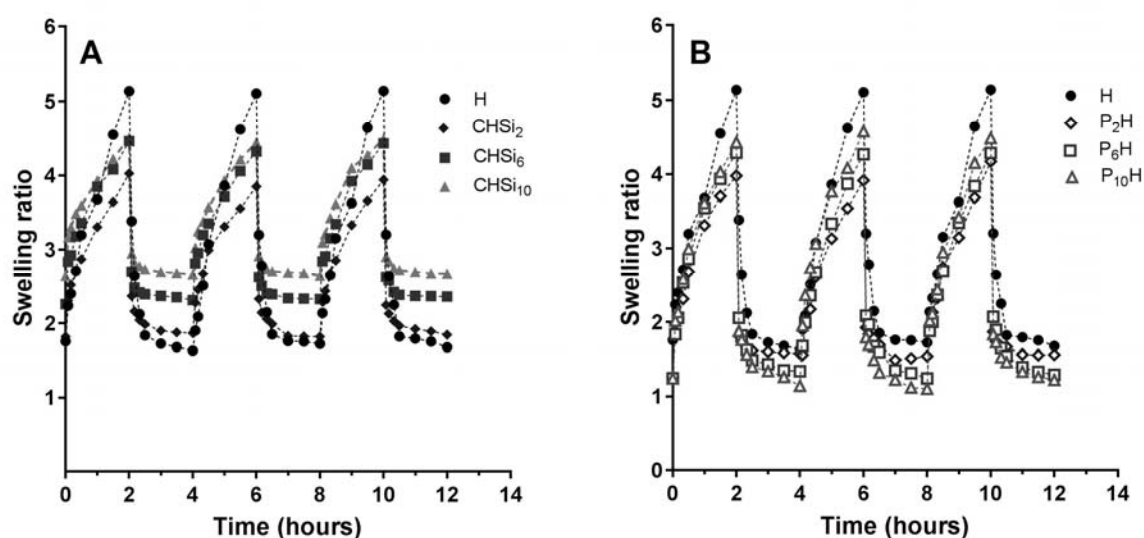


Fig. 6 – Cycles of the swelling/deswelling processes of the composite (A) and porous (B) hydrogels in comparison with conventional one (sample H).

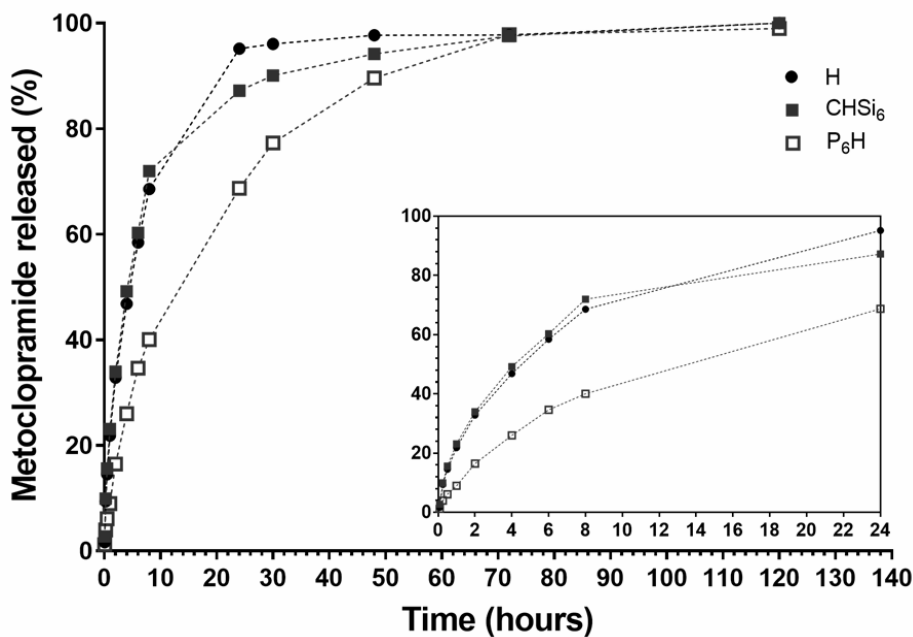


Fig. 7 – Release kinetics of Met from poly(NIPAAm-co-HEAAm) hydrogels in standard phosphate buffer solution of pH=7.4 at 37 °C. For comparison, the release profile of Met from SiMs was represented.

#### 4. *In vitro* release studies

The release kinetics of Met from hydrogels was studied in PBS at pH=7.4, at 37 °C (**Fig. 7**). It is expected that diffusion of Met from hydrogels into the release medium to be controlled by steric interactions between drug and the polymer network, since the polymeric network does not contain ionic groups.

As shown in **Fig. 7**, the release profiles of Met from porous hydrogels exhibit a delayed release pattern in comparison with the fast release from the conventional hydrogel. This behavior can be explained by the fact that over the VPTT, the polymeric network is dehydrated, hydrophobic and collapsed and therefore hinders the diffusion of drug. Moreover, an increased temperature favors hydrophobic interactions between Met and thermosensitive hydrogel. As a result, the release rate is substantially reduced, the total amount of drug being released in 3 days in comparison with one day recorded for conventional hydrogels.

#### CONCLUSIONS

Thermoresponsive poly(NIPAAm-co-HEAAm)/silica composite hydrogels were prepared successfully by the free-radical polymerization of NIPAAm and a suitable cross-linker in the presence of silica microspheres of micrometer size.

After silica extraction in HF, a porous hydrogel was formed. SEM micrographs of dried hydrogels showed the presence of pores, and the density of pores was controlled by the amount of silica particles embedded. Porous hydrogels showed a rapid and controllable swelling/deswelling process. The composite hydrogels presented fast release profiles comparing with conventional hydrogels. However, after removal of silica particles, the porous hydrogel exhibits a delayed release pattern which makes them suitable for controlled drug delivery.

*Acknowledgements:* This publication is part of a project that has received funding from the *European Union's Horizon 2020 research and innovation programme* under grant agreement No. 667387 WIDESPREAD 2-2014 SupraChem Lab. This work was also supported by a grant of the Roumanian National Authority for Scientific Research and Innovation, CNCS/CCCDI – UEFISCDI, project number PN-III-P3-3.6-H2020-2016-0011, within PNCDI III.

#### REFERENCES

1. N. V. Gupta and H. G. Shivakumar, *DARU*, **2010**, *18*, 200-210.
2. A. Salerno, R. Borzacchiello and P. A. Netti, *Appl. Polym. Sci.*, **2011**, *122*, 3651–3660.
3. M. Constantin, M. Cristea, P. Ascenzi and G. Fundueanu, *Express Polym. Lett.*, **2011**, *5*, 839–848.
4. Z. Zhao, Z. Li, Q. Xia, H. Xi and Y. Lin, *Eur. Polym. J.*, **2008**, *44*, 1217–1224.

5. P. E. Jagadeesh Babu, R. S. Kumar and B. Maheswari, *Colloids Surf. A*, **2011**, *384*, 466–472.
6. K. Depa, A. Strachota, M. Šlouf and J. Hromádková, *Eur. Polym. J.*, **2012**, *48*, 1997–2007.
7. X. Z. Zhang and R. X. Zhuo, *Langmuir*, **2001**, *17*, 12–16.
8. T. Asoh, T. Kaneko, M. Matsusaki and M. Akashi, *J. Control. Release*, **2006**, *110*, 387–394.
9. X. Z. Zhang, C. C. Chu and R. X. Zhuo, *J. Polym. Sci. A*, **2005**, *43*, 5490–5497.
10. X. Z. Wu, C. C. Chu and R. X. Zhuo, *J. Polym. Sci. A*, **1992**, *30*, 2121–2129.
11. J. T. Zhang, S. W. Huang and R. X. Zhuo, *Macromol. Biosci.*, **2004**, *4*, 575–578.
12. O. Liu, P. Zhang, A. Qing and M. Lu, *Polymer*, **2006**, *47*, 2330–2336.
13. C. Tang, L. Yin, Y. Pei, M. Zhang and L. Wu, *Eur. Polym. J.*, **2005**, *41*, 557–562.
14. G. Fundueanu, M. Constantin, I. Asmarandei, S. Bucatariu, V. Harabagiu and P. Ascenzi, *Eur. J. Pharm. Sci.*, **2013**, *85*, 614–623.
15. T. Serizawa, K. Wakita and M. Akashi, *Macromolecules*, **2002**, *35*, 10–12.
16. T. Serizawa, K. Wakita, T. Kaneko and M. Akashi, *J. Polym. Sci. A*, **2002**, *40*, 4228–4235.
17. J. H. Kim, S. B. Lee, S. J. Kim and Y. M. Lee, *Polymer*, **2002**, *43*, 7549–7558.

